

Direct Assembly and Tuning of Dynamical Neural Networks for Kinematics

Chloe K. Guie^(⊠) and Nicholas S. Szczecinski D

Department of Mechanical and Aerospace Engineering, West Virginia University, Morgantown, WV 26505, USA

ckg00003@mix.wvu.edu

Abstract. It is unknown precisely how the nervous system of invertebrates combines multiple sensory inputs to calculate more abstract quantities, e.g., combining the angle of multiple leg joints to calculate the position of the foot relative to the body. In this paper, we suggest that non-spiking interneurons (NSIs) in the nervous system could calculate such quantities and construct a neuromechanical model to support the claim. Range fractionated sensory inputs are modeled as multiple integrate-and-fire neurons. The NSI is modeled as a multi-compartment dendritic tree and one large somatic compartment. Each dendritic compartment receives synaptic input from one sensory neuron from the knee and one from the hip. Every dendritic compartment connects to the soma. The model is constructed within the Animatlab 2 software. The neural representation of the system accurately follows the true position of the foot. We also discuss motivation for future research, which includes modeling other hypothetical networks in the insect nervous system and integrating this model into task-level robot control.

Keywords: Non-spiking interneuron \cdot Leaky integrator \cdot Compartmental model \cdot Synthetic nervous system \cdot Functional subnetwork approach \cdot Legged locomotion

1 Introduction

Sensory feedback is critical for the control of legged locomotion in vertebrates and arthropods alike [1]. One hypothesis for how higher-order quantities such as body posture is controlled by the action of many smaller units such as individual joints and muscles is 'task-level control', in which the nervous system presumably issues motor commands at the task level (e.g., a desired foot position in space) and must calculate task-level feedback for comparison [2]. Many mechanical states that would be valuable to control, e.g., the position of the foot in space, cannot be measured directly by the nervous system, and therefore must be calculated by the nervous system using local measurements (e.g., joint angles). However, it is not known how such calculations are performed.

In insects, we hypothesize that local non-spiking interneurons (NSIs) in the thoracic ganglia (ventral nerve cord) may facilitate the calculation of task-level quantities for motor control. Measurements such as joint angles are represented by the activity of many

© The Author(s), under exclusive license to Springer Nature Switzerland AG 2022 A. Hunt et al. (Eds.): Living Machines 2022, LNAI 13548, pp. 321–331, 2022. https://doi.org/10.1007/978-3-031-20470-8_32 distributed sensory neurons, each of which is sensitive to a small range of joint motion, an organizational principle called "range fractionation" [3]. Range fractionation consists of sensory neurons measuring the same state (e.g., joint angle), each with varying firing thresholds for different stimuli intensities. In insects such as the stick insect and locust, these range fractionated afferent neurons synapse onto NSIs, which integrate sensory input from joint angle sensors such as the chordotonal organ (CO) and segment strain sensors such as campaniform sensilla (CS) from across the leg, then synapse onto the motor neurons to contribute to control of the leg [4]. Although it is unclear what task-level calculations each NSI encodes, each appears to act as an information "hourglass" in which information from many range-fractionated sensory neurons converges onto the NSI, then diverges due to NSI synapses onto multiple motor neurons throughout the leg. In this study, we use a neuromechanical model to demonstrate that the NSIs could calculate task-level quantities directly from range-fractionated sensory inputs.

The model we propose could also be used to calculate task-level quantities for robot control. In robotics, task-level quantities may be calculated by the direct application of forward kinematics equations, e.g., through the product of exponentials formulation [5]. More recently, Deep Neural Networks (DNNs) have been trained to compute complicated nonlinear forward kinematics equations [6, 7]. Although this approach has been successful, DNNs can be computationally expensive to tune, making them impractical for some applications. Furthermore, their dense connectivity may not model the structure of the peripheral nervous system, which is exquisitely structured; because we are interested in modeling the nervous system, we seek a system with more direct biological inspiration. These challenges inspire the assembly and tuning of dynamical networks that can mimic the structure and function of the nervous system to perform kinematic calculations.

The goal of this research is to better understand how insects compute task-level quantities by integrating range-fractionated sensory signals. To accomplish this goal, we constructed a biologically plausible model in which spiking afferents from two joints in a leg are integrated by one nonspiking neuron, modeled with many dendritic compartments and one somatic compartment. The voltage of the somatic compartment encodes the x-coordinate of the foot's position relative to the body. Conductances between the compartments are tuned using the Functional Subnetwork Approach (FSA) [8], which has been used in the past to construct and tune rate-coded networks. The current study is the first application of the FSA to construct and tune place-coded networks. Finally, we discuss future opportunities for applying this network structure to model the nervous system or as part of a robot control system.

2 Methods

2.1 Neuron Model

The neuron model was designed using our Synthetic Nervous System (SNS) philosophy. An SNS model is meant to capture as many biological details as possible while running as quickly as possible to facilitate implementation as a robot control system. Thus, the NSI model was constructed from leaky integrator compartments [8]. Spiking neurons

were implemented as generalized leaky integrate-and-fire neurons with conductance-based synapses [9]. Simulation was performed through the neuromechanical simulator AnimatLab 2 [10].

The non-spiking interneuron (NSI) was modeled as 25 low-capacity dendrite compartments that connect to 1 high-capacity soma compartment. Each of the 25 compartments is modeled as a leaky integrator with the dynamics

$$C_{mem} \cdot \dot{U} = -G_{mem} \cdot U + \sum_{i=1}^{n} G_{syn}^{i} \cdot \left(E_{syn}^{i} - U \right) + I_{app}, \tag{1}$$

where U is the compartment's voltage, G_{mem} is the leak conductance of the cell membrane (we set $G_{mem}=1\mu S$ in every case), C_{mem} is the membrane capacitance of that compartment, I_{app} is an optional applied current, n is the number of incoming synapses to that compartment, G_{syn}^i is the instantaneous conductance of the i^{th} incoming synapse, and E_{syn}^i is the reversal potential of the i^{th} incoming synapse relative to the compartment's rest potential. When all incoming synapses have a conductance of 0, the neuron has the time constant $\tau_{mem} = C_{mem}/G_{mem}$; because $G_{mem} = 1\mu S$ in every case, τ_{mem} is directly proportional to C_{mem} .

To simulate the conductance of current from the dendrite to the soma, the compartments were connected by graded-potential synapses, such that

$$G_{syn} = G_{max} \cdot \min(\max(U/R, 0), 1), \tag{2}$$

where G_{max} represents the maximal inter-compartment coupling and R is a constant voltage that represents the expected fluctuation of one compartment's voltage [8].

The joint angle-encoding afferent neurons were modeled as generalized leaky integrate-and-fire neurons. The voltage of each neuron follows the same dynamics as the nonspiking compartments, but with the additional consideration that when the membrane voltage U surpasses the spiking threshold θ , a spike occurs and U is set to 0 in the following time step.

Spiking synapses were modeled as first-order different equations, with the conductance following the dynamics

$$\tau_{syn} \cdot \dot{G}_{syn} = -G_{syn},\tag{3}$$

where τ_{syn} is the decay time constant. When the presynaptic neuron spikes, G_{syn} is set to its maximum value, G_{max} .

2.2 Sensory Model

To demonstrate that the NSIs may compute task-level states of the leg despite being only one or two synaptic connections from the sensory neurons themselves, we constructed a simple kinematic model of a two-jointed planar leg based on the stick insect (Fig. 1A). This leg has a hip joint, which is connected to the origin of the coordinate system, and a knee, which connects the femur and tibia segments. Each segment is 10 cm long. Each joint is limited to rotate between 0.75 rad (43°) and -0.75 rad (-43°). At the distal end of the tibia is the foot, whose position is designated by the point $P = (P_x, P_y)$.

We wished for our test network to encode the x coordinate of the foot's position, P_x , in the voltage of the NSI soma (Fig. 1B). We assumed that each joint angle is represented in a range-fractionated manner by five sensory neurons, although single joint sensing organs may possess hundreds of sensory neurons [11]. Each neuron receives an applied current based on the instantaneous joint angle θ ,

$$I_{app}(\theta) = R \cdot \exp(-c \cdot (\theta - b)^2), \tag{4}$$

where R is the amplitude, b is the mean value, and c controls the width of the Gaussian bell curve. In our model, R=20 nA. In our model, each hip sensory neuron had a unique value of b, equally spaced between the minimum (-0.75 rad [-43°]) and maximum (0.75 rad [43°]) angles of the joint (see diagrams in Fig. 1B). The knee sensory neurons were configured in the same way. Finally, parameter c was varied logarithmically between values of 7.5 and 60 to test its effect on the network's encoding accuracy.

Each sensory neuron was designed such that its spiking frequency was proportional to the Gaussian applied current I_{app} using the methods in [9]. In short, given a maximum input current of 20 nA and a desired maximum spiking frequency of 100 Hz, the parameter values in Eq. 1 could be determined. In our model, $C_{mem} = 200$ nF, $G_{mem} = 1 \mu S$ (resulting in a time constant of 200 ms), $\theta = 1$ mV, and each neuron receives a tonic applied current of 0.5 nA in addition to I_{app} from Eq. 4.

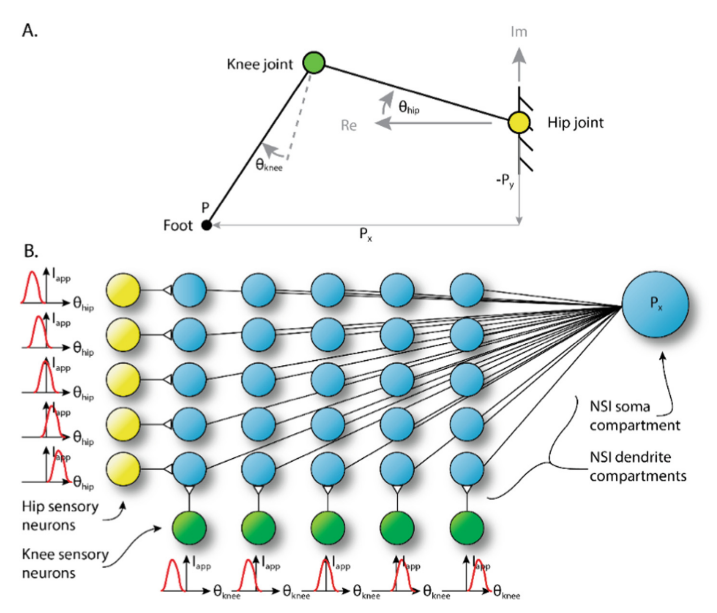


Fig. 1. (A) Schematic of a planar leg with a hip joint and a knee. The angle of rotation to the global real axis is defined by θ_{hip} or θ_{knee} . (B) Schematic of the sensory neurons from hip, the yellow circles, and knee, the green circles. One of each the hip and knee sensory neurons excites the NSI dendrite compartments in its row or column, respectively. Every NSI dendrite compartment, the smaller blue circles, then connects to the NSI soma compartment, the large blue circle, creating a unique conductance value that represents the diameter of each of the bell curves.

The network was structured such that each NSI dendrite compartment received excitatory synaptic input from exactly one hip sensory neuron and exactly one knee sensory neuron, reflected in the grid structure of Fig. 1B. Each dendrite compartment then made a connection to the soma with a unique conductance value. These varying conductance values represent the varying diameter of the dendritic structure of the NSI.

2.3 Tuning Parameters Within the Model

To tune the network parameter values, we first needed to calculate the ground-truth position to be encoded, P_x , the x coordinate of the foot's position. Because the leg model is planar, we can represent the position of the foot relative to the origin using complex number vector notation. Each vector is represented as a complex number, with the real component indicating the x coordinate and the imaginary component indicating the y coordinate. Rotations are performed by multiplying by $\exp(j\theta)$, in which $j = \sqrt{-1}$ and θ is the angle of rotation relative to the global real axis. Using this notation and the angles as defined in Fig. 1A,

$$P_x = \text{Re}\left(L \cdot \exp(j\theta_{hip}) + L \cdot \exp\left(j \cdot \left(\theta_{hip} + \theta_{knee} - \frac{\pi}{2}\right)\right)\right),\tag{5}$$

where Re is the real component of the result, L is the length of the femur and the tibia, θ_{hip} is the angle between the ground and the femur, and θ_{knee} is the angle between the femur and knee, with a $\pi/2$ radian offset. Plotting P_x versus θ_{hip} and θ_{knee} produces a surface of the foot position's dependence on the locally-measured joint angles that the network encodes (Fig. 2).

The lateral foot position P_x was mapped to the conductance values from each dendrite compartment to the soma. In this way, the soma voltage was driven to a value that reflected P_x simply due to the structure and tuning of the conductance values. Specifically, we applied the Functional Subnetwork Approach [8] by mapping the value of P_x for each pair of θ_{hip} and θ_{knee} values to the gain k of the conductance from the dendrite compartment to the soma compartment:

$$k = \frac{P_x - \min(P_x)}{\max(P_x) - \min(P_x)}.$$
 (6)

Then, the corresponding conductance g could be calculated using R = 20 mV, the maximum expected membrane voltage above rest, and E = 70 mV, the reversal potential above the resting membrane potential,

$$g = \frac{k \cdot R}{E - k \cdot R}.\tag{7}$$

The resulting conductance value from each dendrite to the soma is plotted in Fig. 2. This conductance value surface is reminiscent of the lateral foot position surface but is ultimately different due to the difference in units and the nonlinear nature of Eq. 7.

To compare the membrane voltage of the soma to the actual foot position, we calculated the expected neural encoding of P_x as

$$U_{exp} = k \cdot R, \tag{8}$$

where k is defined in Eq. 6 and R = 20 mV.

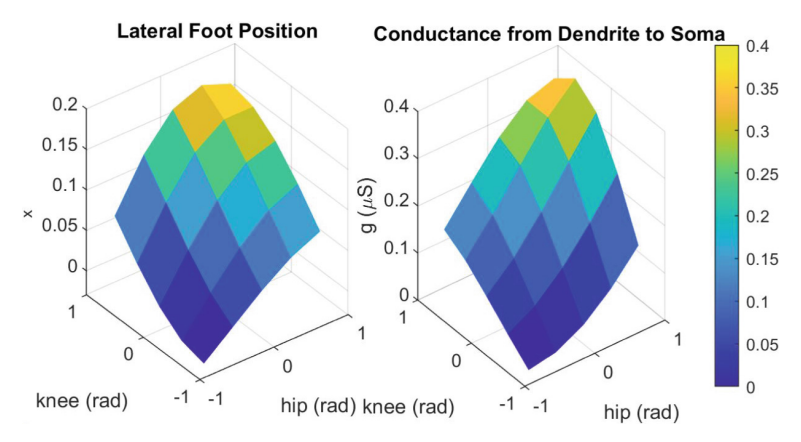


Fig. 2. From left to right respectively, a surface plot of the lateral foot position versus the knee and hip joint angles and a surface plot of the conductance from the dendrite to the soma versus the knee and hip joint angles.

3 Results

To test how well our model NSI could encode foot position, the hip and knee angles were cycled at different frequencies to sample many different combinations of angle

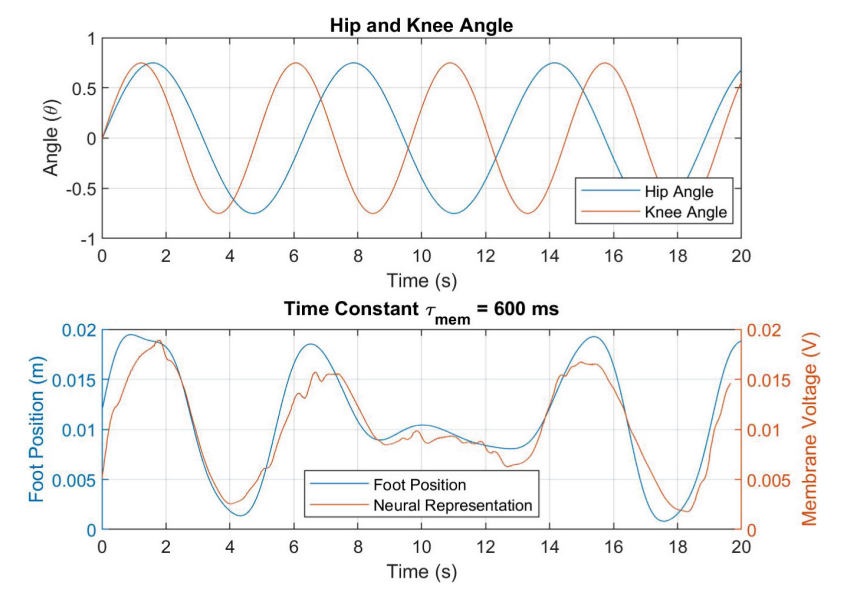


Fig. 3. Top, a plot of the hip and knee angles versus time. Bottom, a plot of the position of the foot and the neural representation versus time with the Gaussian function width c=15 and the time constant $\tau_{mem}=600$. Note that the neural representation has been advanced in time as calculated by cross-correlation between the curves.

values. Figure 3 compares the encoded foot position (U_{exp} in Eq. 8) and the neural representation of the foot position versus time during such a test. This plot shows that the neural representation tracks the position of the foot. The system works reasonably accurately with the Gaussian function width c = 15 for the sensory neurons and the soma's time constant $\tau_{mem} = 600ms$ (i.e., $C_{mem} = 600$ nF).

We sought to understand how the parameters within this network affect the accuracy and time lag of the neural representation of the foot position relative to the expected value. Altering the width c in the Gaussian function from Eq. 4 affected the offset of the soma's membrane voltage. Figure 4 shows that if each sensory neuron's response curve is too narrow, e.g., the width c=30 in each Gaussian function, the soma's voltage level is lower than expected. This occurs because there are "dead zones" in which no sensory neurons are spiking as the joints rotate, and the dendrite and soma compartments leak their current. In contrast, Fig. 5 shows that if each sensory neuron's response curve is too wide, e.g., the width c=7.5 in each Gaussian function, the soma's voltage level is higher than expected. This occurs because several sensory neurons are active at once, exciting many dendrite compartments and consequently overexciting the soma.

Altering the time constant of the soma (proportional to C_{mem} from Eq. 1) decreased the soma's response magnitude and introduced lag in the neural representation of the foot position. Figure 6 shows a case where c=15 and $\tau=6000$ ms. The fluctuations in the neural representation lag behind the true foot position by almost 2 s, which is likely too long to be useful for closed-loop leg control. This motivates finding the lowest possible value for τ that preserves accurate encoding of the foot position.

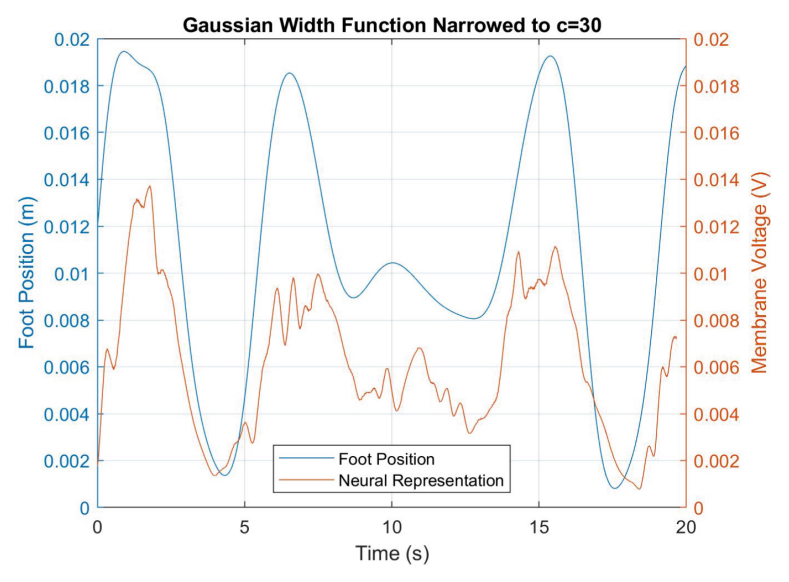


Fig. 4. A plot of the position of the foot and the neural representation versus time with the width 30 and the time constant 600 ms. This shows that by narrowing the width, the neural representation's amplitude decreases.

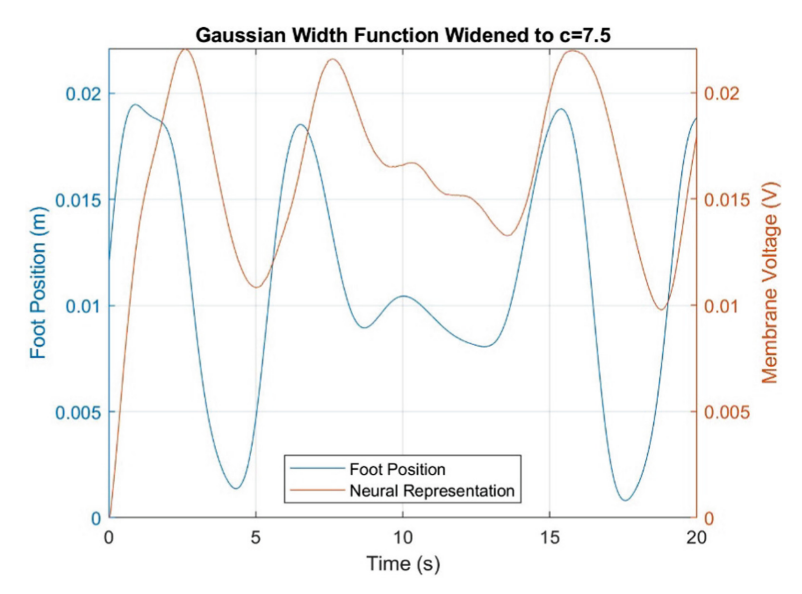


Fig. 5. A plot of the position of the foot and the neural representation versus time with the width 7.5 and the time constant 600 ms. This shows that by widening the width, the neural representation's amplitude decreases and its mean value is shifted upward.

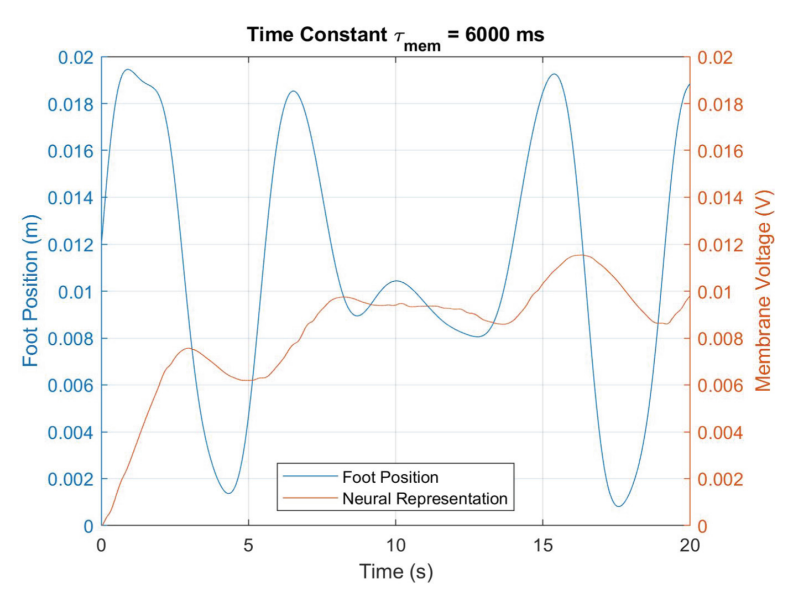


Fig. 6. A plot of the position of the foot and the neural representation versus time with the width 15 and the time constant 6000. This shows that by lengthening the time constant, the neural representation lags behind the foot position.

To better understand trends in the network performance as its parameter values change, we calculated the mean absolute error between the foot position and neural representation for multiple values of c, the width of the sensory encoding curve from Eq. 4. Figure 7 (A) plots mean absolute error between the expected and actual network activity throughout one trial *versus* the different widths, clearly demonstrating that for this leg motion, c = 15 minimizes the error of foot position encoding. We also calculated the lag of the neural representation relative to the foot position by finding the shift in time necessary to maximize the cross correlation between the signals. Figure 7 (B) plots the lag versus the time constant. The plot clearly shows that increasing the time constant increases the lag of the neural representation.

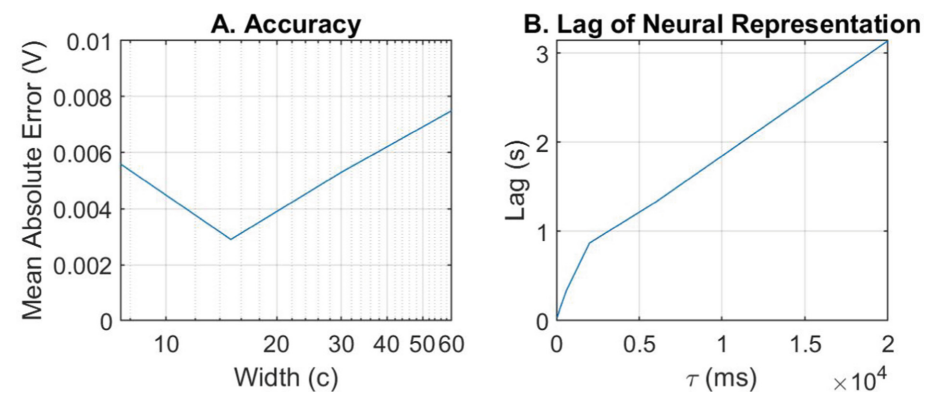


Fig. 7. A. A plot of the accuracy of the system. The system operates the most accurately when the width c = 15. When the width is changed in either direction, the system works less accurately. B. A plot of the lag of the system versus the time constant. This shows that the longer the time constant of the soma compartment, the longer the lag between the foot position and the soma's voltage. To decrease the lag, τ should be as small as possible.

4 Discussion

Although it is unknown, we discussed that higher-order quantities may be calculated by the nervous system through the use of many local measurements. We model how local NSIs of insects may calculate different quantities for motor control. In our model, range fractionated sensory inputs impinge onto multiple compartments that simulate the dendrite of the NSI. Each compartment is coupled to the soma with a different conductance value that reflects the mechanical quantity to be encoded (in this study, the x component of the foot's position in space). We modeled this using our Synthetic Nervous System philosophy to create and tune a dynamical network. For our system, we found parameter values for which the neuron's voltage encoded the position of the foot closely. We found that the performance of the network depended on the width of the sensory encoding curves (Eq. 4) and the time constant of the soma τ_{mem} (proportional to C_{mem} in Eq. 1).

We argue that models of nervous system processing of sensory information may be more accurate if they include range fractionated inputs. However, this is not commonly done. One study from Ache and Dürr demonstrated the power of range fractionated inputs by identifying and modeling descending interneurons (DINs) from the antennae to the thoracic networks of the stick insect *Carausius morosus* [12]. In their model, DINs integrated input from many range fractionated sensory neurons to calculate higher order "codings" of the antennae movement, e.g., their positions and velocities. Our study pursues a similar goal, to calculate the position of the foot from multiple range-fractionated measurements of several joints' angles. The diversity of DIN responses and the success of Ache and Dürr's model suggests that we can apply our method to calculate other features of leg motion, e.g., foot velocity, manipulator Jacobian of the leg.

There are several opportunities to expand and improve the model from this study. One simplification we made was to assume this is a small network, with only five sensory neurons sensing the hip angle and five sensory neurons sensing the knee angle. In reality, insect joint sensors have many more sensory neurons [11], and the neurons may encode diverse features of motion [3]. However, our simplified network demonstrated that this approach could be applied to calculate leg kinematics from multiple joint angle measurements. In the future, we plan to investigate how the joints' range of motion and the accuracy of network encoding depend on the number of sensory neurons.

Another simplification we made in our model was to configure the conductances from the dendrite compartments to the soma compartment such that current could only flow from the dendrite to the soma. Such a simplification eliminated the coupling between dendritic compartments and simplified network tuning. In reality, NSIs have large branching structures through which current may flow in any direction and may not directly excite the soma [13–15]. We have begun to apply the lessons learned from this study to construct more realistic NSI models, in which adjacent dendritic compartments are coupled and current can flow in any direction. We suspect that increasing the realism of our model will produce a computational unit whose function is highly resilient in the face of incomplete sensory feedback.

Another opportunity to expand this framework is to construct networks that calculate quantities other than forward kinematics for a simple leg model. To more broadly test the application of the Functional Subnetwork Approach to tuning models of this type (i.e., many-to-one mappings), we plan to build networks that calculate other quantities, such as the manipulator Jacobian, as noted above. Should this method prove broadly applicable, we plan to use it to construct transparent models of networks that incorporating the whole-limb and whole-body feedback for both leg-local control and ascending sensory signals to the brain.

Acknowledgements. This work was supported by NSF IIS 2113028 as part of the Collaborative Research in Computational Neuroscience Program. This work was also supported by NSF DBI 2015317 as part of the NSF/CIHR/DFG/FRQ/UKRI-MRC Next Generation Networks for Neuroscience Program.

References

- Buschmann, T., Ewald, A., Twickel, A. von, Büschges, A.: Controlling legs for locomotion -Insights from robotics and neurobiology. Bioinspiration and Biomimetics. 10, (2015). https://doi.org/10.1088/1748-3190/10/4/041001
- Safavynia, S.A., Ting, L.H.: Sensorimotor feedback based on task-relevant error robustly predicts temporal recruitment and multidirectional tuning of muscle synergies. J Neurophysiol. 109, 31–45 (2013). https://doi.org/10.1152/jn.00684.2012.-We
- 3. Delcomyn, F., Nelson, M.E., Cocatre-Zilgien, J.H.: Sense organs of insect legs and the selection of sensors for agile walking robots. The International Journal of Robotics Research. 15, 113–127 (1996). https://doi.org/10.1177/027836499601500201
- Gebehart, C., Schmidt, J., Büschges, A.: Distributed processing of load and movement feedback in the premotor network controlling an insect leg joint. J Neurophysiol. 125, 1800–1813 (2021). https://doi.org/10.1152/jn.00090.2021
- Murray, R.M., Li, Z., Sastry, S.S.: A Mathematical Introduction to Robotic Manipulation. CRC Press (2017). https://doi.org/10.1201/9781315136370
- Su, H., Qi, W., Yang, C., Aliverti, A., Ferrigno, G., de Momi, E.: Deep neural network approach in human-like redundancy optimization for anthropomorphic manipulators. IEEE Access. 7, 124207–124216 (2019). https://doi.org/10.1109/ACCESS.2019.2937380
- Sandbrink, K.J., Mamidanna, P., Michaelis, C., Mathis, M.W., Bethge, M., Mathis, A.: Task-driven hierarchical deep neural network models of the proprioceptive pathway. https://doi.org/10.1101/2020.05.06.081372
- Szczecinski, N.S., Hunt, A.J., Quinn, R.D.: A functional subnetwork approach to designing synthetic nervous systems that control legged robot locomotion. Frontiers in Neurorobotics. 11 (2017). https://doi.org/10.3389/fnbot.2017.00037
- Szczecinski, N.S., Quinn, R.D., Hunt, A.J.: Extending the functional subnetwork approach to a generalized linear integrate-and-fire neuron model. Frontiers in Neurorobotics. 14 (2020). https://doi.org/10.3389/fnbot.2020.577804
- Cofer, D., Cymbalyuk, G., Reid, J., Zhu, Y., Heitler, W.J., Edwards, D.H.: AnimatLab: A 3D graphics environment for neuromechanical simulations. J. Neurosci. Methods 187, 280–288 (2010). https://doi.org/10.1016/j.jneumeth.2010.01.005
- Mamiya, A., Gurung, P., Tuthill, J.C.: Neural coding of leg proprioception in drosophila. Neuron 100, 636-650.e6 (2018). https://doi.org/10.1016/j.neuron.2018.09.009
- Ache, J.M., Dürr, V.: A computational model of a descending mechanosensory pathway involved in active tactile sensing. PLoS Computational Biology. 11 (2015). https://doi.org/ 10.1371/journal.pcbi.1004263
- Burrows, M.: Inhibitory Interactions Between Spiking and Nonspiking Local Interneurons in the Locust (1987)
- 14. Pearson, K.G., Fourtner, C.R.: Nonspiking Interneurons in Walking System of the Cockroach
- Smarandache-Wellmann, C.R.: Arthropod neurons and nervous system (2016). https://doi. org/10.1016/j.cub.2016.07.063